

A comparison of the gamma-ray bursts detected by BATSE and Swift

D. Huja¹, A. Mészáros¹, and J. Řípa¹

Charles University, Faculty of Mathematics and Physics, Astronomical Institute, V Holešovičkách 2, 180 00 Prague 8, Czech Republic
e-mail: David.HUJA@seznam.cz
e-mail: meszaros@cesnet.cz
e-mail: ripa@sirrah.troja.mff.cuni.cz

Received March 18, 2008; accepted May 22, 2009

ABSTRACT

Aims. The durations of 388 gamma-ray bursts, detected by the Swift satellite, are studied statistically in order to search for their subgroups. Then the results are compared with the results obtained earlier from the BATSE database.

Methods. The standard χ^2 test is used.

Results. Similarly to the BATSE database, the short and long subgroups are well detected also in the Swift data. Also the intermediate subgroup is seen in the Swift database.

Conclusions. The whole sample of 388 GRBs gives a support for three subgroups.

Key words. gamma-rays: bursts

1. Introduction

In the years 1991-2000 2704 gamma-ray bursts (GRBs) were detected by the BATSE instrument onboard the Compton Gamma-Ray Observatory (Meegan et al. 2001). After the launch of the Swift satellite (November 2004) the frequency of detected GRBs by this instrument is cca 100/year (Gehrels et al. 2005). Trivially, any comparison of different databases is highly useful. For example, in the BATSE database - doubtlessly - three subgroups ("short", "intermediate" and "long" GRBs) are seen (Horváth et al. 2006, Chattopadhyay et al. 2007 and references therein). The short and long subgroups are physically different phenomena (Balázs et al. 2003). However, contrary to this, it is still well possible that the intermediate subgroup is not a real physically different separate subgroup and it is occurring in the BATSE database due to e.g. some observational biases arising from the BATSE triggering procedure (Horváth et al. 2006). The best choice, to proceed in this "bias vs. separate subgroup" controversy, is a new study of another database gained by another instrument. Hence, it is highly useful to ask: Are these subgroups also seen in the Swift data-set?

The purpose of this article is the statistical analysis of the Swift database, which could answer this question. We will proceed identically to the successful statistical analysis done on the BATSE Catalog (Horváth 1998) leading to the discovery of the third subgroup (Mukherjee et al. 1998, Bagoly et al. 1998, Horváth 1999, Hakkila et al. 2000, Rajaniemi & Mähönen 2002, Horváth 2002, Horváth 2003, Balázs et al. 2003, Horváth et al. 2006, Chattopadhyay et al. 2007). Recently, a statistical study on the Swift database - using the

maximum likelihood method - has already shown evidence for the third subgroup (Horváth et al. 2008). The χ^2 fitting was not used, "because of the small population". However, historically, the first evidence for the third subgroup in the BATSE database came just from the χ^2 method (Horváth 1998), and also the number of 388 need not be small for this testing. Hence, in any case, one has to probe this fitting on the Swift data sample too. In addition, since approximately one third of the Swift's bursts have already well determined redshifts (contrary to the BATSE's GRBs, where only a few objects had measured redshifts (Ramirez-Ruiz & Fenimore 2000, Norris 2002, Bagoly et al. 2003)), some additional tests can be also done on the samples with and without redshifts.

The paper is organized as follows. The samples are defined in Section 2 - these samples are also listed in detail at the end of the article. Section 3 presents the χ^2 fitting of these samples. Section 4 discusses the results of this paper and Section 5 summarizes them.

2. The samples

We define two samples from the Swift data-set (Gehrels et al. 2005): the sample of GRBs without measured redshifts (z) and the sample with measured redshifts. These two samples are collected in Tables 4-8 and Tables 9-11, respectively. We compiled these tables for the convenience; each table contains the name of GRB, its BAT duration T_{90} , BAT fluence at range 15 – 150 keV, BAT 1-sec peak photon flux at range 15 – 150 keV and Tables 9-11 also redshift. Only these bursts were taken into account, of which the GRB duration was measured. The samples cover the period from November 2004 to the end of February 2009; the first (last) object is GRB041217

Table 1. Results of the χ^2 fitting of the whole sample with 388 GRBs.

<i>Fit</i>	<i>I.</i>	<i>II.</i>	<i>III.</i>	<i>IV.</i>	<i>V.</i>	<i>VI.</i>	<i>VII.</i>
<i>No. of bins</i>	30	34	35	36	25	15	31
1G							
χ^2_1	90.5	105.6	97.4	112.3	97.5	56.6	94.5
<i>si.</i> [%]	10^{-6}	10^{-8}	10^{-6}	10^{-8}	10^{-9}	10^{-5}	10^{-7}
μ	1.45	1.52	1.45	1.45	1.45	1.47	1.44
σ	0.87	0.88	0.89	0.87	0.93	0.83	0.89
2G							
χ^2_2	30.9	40.1	31.3	47.7	17.3	7.5	23.1
<i>si.</i> [%]	15.6	6.5	34.4	2.1	58.8	58.6	57.1
μ_1	0.48	0.46	0.41	0.32	0.06	0.42	0.33
σ_1	0.93	0.99	0.98	0.95	1.09	0.92	0.97
μ_2	1.63	1.68	1.62	1.61	1.60	1.62	1.62
σ_2	0.51	0.52	0.52	0.53	0.54	0.53	0.52
w_2	0.84	0.76	0.85	0.88	0.85	0.83	0.82
<i>F</i> [%]	10^{-3}	10^{-4}	10^{-5}	10^{-4}	10^{-5}	10^{-2}	10^{-6}
3G							
χ^2_3	21.4	29.7	22.6	35.9	10.0	2.4	16.7
<i>si.</i> [%]	43.6	23.7	65.5	11.6	86.7	88.2	78.0
μ_1	0.34	0.91	0.11	0.19	-0.01	1.07	0.28
σ_1	0.94	1.27	0.98	0.91	1.13	0.97	0.97
μ_2	1.19	1.18	1.24	1.04	1.06	1.12	1.62
σ_2	0.39	0.36	0.45	0.32	0.35	0.53	0.52
w_2	0.35	0.28	0.44	0.26	0.29	0.30	0.18
μ_3	1.91	1.93	1.94	1.84	1.85	1.84	1.84
σ_3	0.36	0.34	0.35	0.38	0.37	0.33	0.38
w_3	0.47	0.47	0.42	0.60	0.56	0.60	0.58
<i>F</i> [%]	4.04	4.66	3.07	4.50	2.52	3.63	5.41

(GRB090205). Tables 4-8 (9-11) contain 258 (130) GRBs, and hence the total number of GRBs, which are studied in this paper, is 388.

In what follows, we study both samples separately and also together as one single set ("the whole sample").

3. χ^2 fitting of the durations

3.1. The whole sample

Since the χ^2 fitting of the GRB duration distribution and the F-test were successfully used in the work Horváth (1998) (presenting the first evidence of the existence of three GRB subgroups), we proceed identically, but with the Swift's data.

The whole sample consists of 388 events having measured T_{90} . We have fitted the histogram of their decimal $\log T_{90}$ values seven times (fits I.-VII.). The results are collected in Table 1, and the fit No.VI. is seen on Fig. 1. We choose different binnings for different fittings with different numbers of bins, with different edges of bins, etc. Also the widths of bins are different. We only require that in each bin the theoretically expected number of GRBs should be higher than 5.

At first, the histogram is fitted with one single theoretical Gaussian curve having two free parameters (mean μ and standard deviation σ). The best parameters giving the minimal χ^2 are, e.g., for fit No.VI. the following ones: $\mu = 1.47$, $\sigma = 0.83$ with $\chi^2_1 = 56.6$. The goodness-of-fit for $15 - 2 - 1 = 12$ degrees of freedom (dof) gives

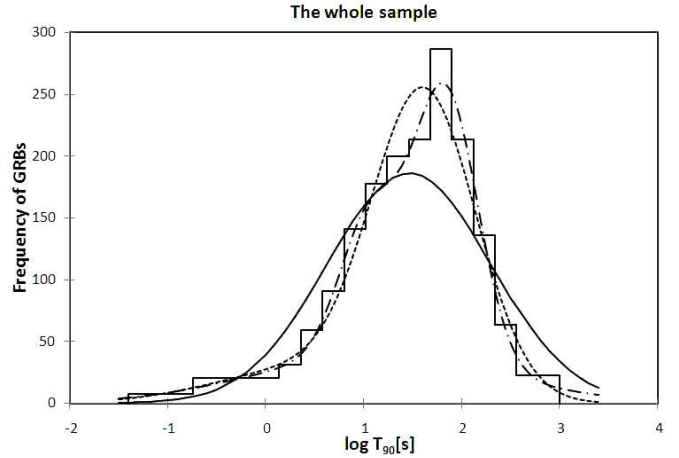


Fig. 1. Fitting of the $\log T_{90}$ histogram in the whole sample with 15 bins (fit No.VI.). The number of GRBs per bin is given by the product of the frequency and width. (There are two equally populated bins between $-0.74 < \log T_{90} < 0.14$ divided at $\log T_{90} = -0.30$. For these bins the frequencies are 20.45, and hence the number of GRBs in these bins equal to $20.45 \times 0.44 = 9$.) The theoretical curves show the best fits: full line = 1 Gaussian curve; dotted line = sum of 2 Gaussian curves; dash-dotted line = sum of 3 Gaussian curves.

the rejection on the level $10^{-5}\%$ (Trumpler & Weaver 1953, Kendall & Stuart 1973). This stands for the rejection of the null-hypothesis (i.e. that one Gaussian curve is enough) that it is correct, because the probability of the mistake for this rejection is not higher than $10^{-5}\%$. The whole sample cannot be described by one single Gaussian curve. The same is the situation also for the remaining six fittings.

The fitting with the sum of two Gaussian curves (five free parameters: two means, two standard deviations and one weight w_2 (since the first weight is equal to $1 - w_2$)) gave for the fit No.VI. $\chi^2 = 7.5$. (Note that the value of w_2 involves that 17% (83%) of GRBs should belong to the short (long) subgroup.) Here dof = $15 - 5 - 1 = 9$ and we obtained an excellent fit with the significance level 58.6% (i.e., if we suppose that the fit is incorrect, then the probability that this assumption is wrong is higher than 58.6%). The assumption that the duration distribution is represented by the sum of two Gaussian curves cannot be - from the statistical point of view - rejected. The best fitted curve is also seen on Fig.1, showing a good correspondence with measured data. Again, the remaining six fits gave similar results.

We also performed the fitting with the sum of three Gaussian curves (eight parameters: three means, three standard deviations and two independent weights), and obtained an excellent fit with $\chi^2_3 = 2.4$ for fit No.VI, because the goodness-of-fit gives for dof = $15 - 8 - 1 = 6$ the significance level is 88.2%. The best fitted curve is also seen on Fig. 1 showing even better correspondence with the measured data. The same excellent fits are obtained also for the remaining six binnings.

The key question here is following: Is the decreasing $\Delta\chi^2 = 7.5 - 2.4 = 5.1$ statistically significant? To answer this question we proceed similarly to Horváth (1998) and used the test proposed by Band et al. (1997) in Appendix A. The significance level from the F-test is 3.63%. This im-

Table 2. Results of the χ^2 fitting of the sample with the known redshift with 130 GRBs.

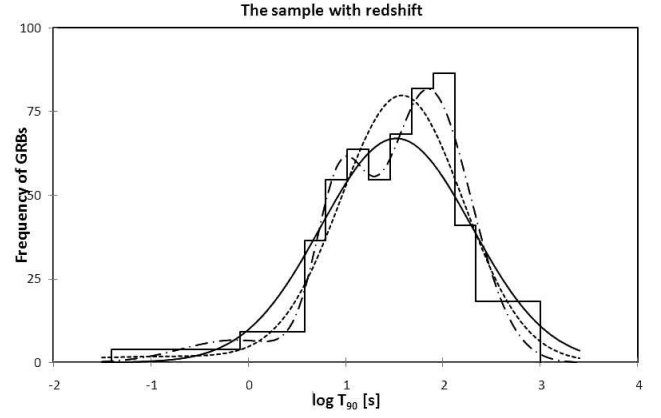
<i>Fit</i>	<i>I.</i>	<i>II.</i>	<i>III.</i>	<i>IV.</i>	<i>V.</i>	<i>VI.</i>	<i>VII.</i>
<i>No. of bins</i>	10	11	12	15	16	17a	17b
1G							
χ^2_1	9.7	12.2	13.9	11.8	14.8	16.8	11.9
<i>si.</i> [%]	20.9	14.4	12.6	46.0	31.8	26.5	61.2
μ	1.55	1.52	1.53	1.69	1.54	1.54	1.53
σ	0.74	0.77	0.74	0.78	0.76	0.75	0.76
2G							
χ^2_2	2.6	6.7	7.7	4.7	7.9	10.1	5.3
<i>si.</i> [%]	62.4	24.0	26.0	86.0	64.0	51.8	91.8
μ_1	1.47	-0.50	0.17	0.22	0.70	-0.69	-0.66
σ_1	0.77	1.00	0.88	0.94	0.86	0.10	0.15
μ_2	1.97	1.58	1.62	1.77	1.68	1.59	1.58
σ_2	0.10	0.63	0.58	0.60	0.55	0.62	0.63
w_2	0.12	0.97	0.91	0.91	0.82	0.97	0.97
<i>F</i> [%]	6.97	28.21	22.19	2.20	6.50	9.74	1.70
3G							
χ^2_3	2.0	2.0	1.9	2.2	4.0	5.4	2.8
<i>si.</i> [%]	15.4	49.8	59.1	89.9	77.8	71.4	94.8
μ_1	1.04	-0.13	1.16	0.17	1.07	-0.57	-0.12
σ_1	0.30	1.00	1.05	0.50	0.92	0.05	0.14
μ_2	1.17	0.94	1.61	1.14	1.32	1.12	0.95
σ_2	1.10	0.26	0.25	0.26	0.12	0.42	0.33
w_2	0.25	0.24	0.53	0.24	0.49	0.48	0.28
μ_3	1.94	1.85	1.91	2.00	1.88	2.00	1.86
σ_3	0.34	0.44	0.18	0.43	0.33	0.34	0.43
w_3	0.49	0.69	0.25	0.67	0.41	0.49	0.67
<i>F</i> [%]	89.64	24.41	10.51	13.29	12.66	11.40	10.96

plies that the rejection of the null-hypothesis (i.e. that the sum of the two Gaussian curves is enough) is adequate, because the probability of the mistake for this rejection is not higher than 3.63%. We arrive into a conclusion that the strengthening of χ^2 need not be a fluctuation. Similar results are obtained for the remaining six fits - only for the fit No.VII the significance is just above the usual 5% limit. (The significances smaller than 5% are denoted by bold-face.) In other words, the introduction of the third subgroup - purely from the statistical point of view - is significant in six fits from the done seven ones. Note that the same F-test can be applied also for the difference $\chi^2_1 - \chi^2_2$, and we always obtain the conclusion that the introduction of the second subgroup - instead of the one single group - is strongly supported.

3.2. The sample with z

The sample contains 130 events with duration informations. Also here we performed seven fits, but now the number of bins needed to be smaller due to the smaller number of objects in the sample. Again we did different binnings - fits VI. and VII. had 17 bins, but the structure was different. In each bin again the number of GRBs was higher than 5. The results are collected in Table 2., and fit No.II. is shown on Fig. 2.

Here the results, compared with the whole sample, are different from two reasons. First, here the fittings with one

**Fig. 2.** Fitting of $\log T_{90}$ in the sample with known redshifts. The theoretical curves show the best fits. The notation of the lines is the same as in Fig.1.**Table 3.** Results of the χ^2 fitting of the sample without the known redshift with 258 GRBs.

<i>Fit</i>	<i>I.</i>	<i>II.</i>	<i>III.</i>	<i>IV.</i>	<i>V.</i>	<i>VI.</i>	<i>VII.</i>
<i>No. of bins</i>	11	14	16	18	20	22	23
1G							
χ^2_1	57.8	66.8	67.3	71.4	76.0	83.8	76.2
<i>si.</i> [%]	10^{-7}	10^{-8}	10^{-7}	10^{-7}	10^{-7}	10^{-8}	10^{-6}
μ	1.47	1.41	1.41	1.41	1.41	1.42	1.41
σ	0.83	0.90	0.86	0.90	0.87	0.90	0.88
2G							
χ^2_2	6.9	9.5	15.1	13.7	18.2	23.2	19.5
<i>si.</i> [%]	22.8	30.6	13.0	31.8	20.0	10.9	30.0
μ_1	-0.04	0.09	0.36	0.22	0.38	0.28	0.48
σ_1	0.81	1.07	0.98	1.06	1.00	1.03	1.03
μ_2	1.58	1.60	1.60	1.61	1.62	1.62	1.63
σ_2	0.51	0.51	0.49	0.50	0.48	0.49	0.48
w_2	0.86	0.83	0.80	0.81	0.79	0.80	0.76
<i>F</i> [%]	0.36	0.04	0.07	0.01	0.01	0.01	10^{-3}
3G							
χ^2_3	2.9	3.1	10.6	9.2	14.8	18.3	17.0
<i>si.</i> [%]	23.3	68.2	15.8	42.1	19.1	14.5	25.9
μ_1	-0.46	-0.55	-0.52	-0.38	0.97	-0.38	-0.12
σ_1	0.40	0.82	0.59	0.80	1.13	0.78	0.86
μ_2	0.86	1.47	1.37	1.51	1.15	1.48	1.52
σ_2	0.33	0.56	0.57	0.57	0.19	0.56	0.55
w_2	0.20	0.77	0.67	0.78	0.17	0.74	0.74
μ_3	1.72	1.97	1.89	1.91	1.82	1.94	1.88
σ_3	0.43	0.15	0.28	0.15	0.29	0.20	0.20
w_3	0.72	0.13	0.25	0.11	0.45	0.15	0.13
<i>F</i> [%]	40.20	6.81	39.50	23.87	47.00	33.60	53.60

single Gaussian curve are also acceptable, and only for two fits the F-test show that the introduction of the second subgroup is adequate. Second, the introduction of the third subgroup is not needed from the F-test. All this shows that this sample can be defined by one single group, and even the separation into the short-long GRBs is not needed.

3.3. The sample without z

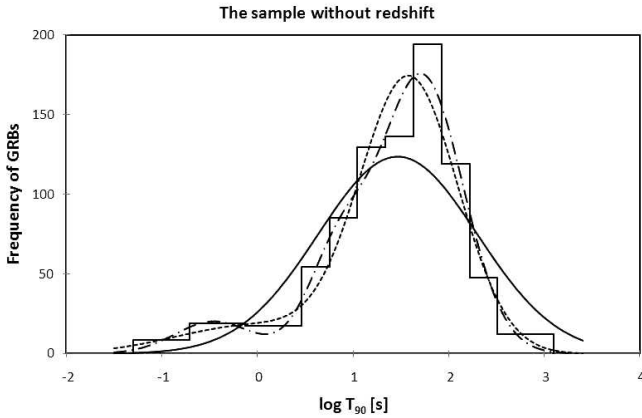


Fig. 3. Fitting of $\log T_{90}$ in the sample with unknown redshifts. The theoretical curves show the best fits. The notation of the lines is the same as in Fig.1.

Here the sample contains 258 events with duration information. Also here we did seven fits with different binnings. In each bin again the number of GRBs was higher than 5. The results are collected in Table 3., and fit No.I. is shown on Fig. 3.

The results, compared with the whole sample, are similar - except for one thing: The introduction of the third subgroup is not needed from the F-test. All this shows that this sample can well be defined by the sum of two and only two subgroups.

4. Discussion of the results

To discuss the results, first of all, we should recognize that we have proven the existence of the short and long subgroups also in the Swift data-set. Both the whole sample and the sample with no redshifts, respectively, contain these two subgroups, because the fits with one single Gaussian curve are fully wrong. It is also highly remarkable that also the weight of the short subgroup is in accordance with the expectation. As it follows from Horváth et al. (2006), in the BATSE Catalog the populations of the short, intermediate and long bursts are roughly in the ratio 20:10:70. Nevertheless, because the short bursts are harder and Swift is more sensitive to softer GRBs, one may expect that in the Swift database the population of short GRBs should be comparable or smaller than 20% due to instrumental reasons. The obtained weights for the whole sample (being between 10 and 26%) are in accordance with this expectation. Also the other values of the best parameters - i.e. two means and two standard deviations - are roughly in the ranges that can be expected from the BATSE values. The differences can be given by the different instrumentations. For example, the mean values of the $\log T_{90}$ should be slightly longer in the Swift database compared with the BATSE data (Barthelmy et al. 2005, Band 2006). In Horváth (1998) the BATSE's means are -0.35 (short) and 1.52 (long), respectively. Here we obtained for the whole sample values from -0.01 to 0.91 (short) and from 1.60 to 1.94 (long), respectively. All this implies that - concerning the short and long GRBs - the situation is in essence identical to the BATSE data-set.

For the sample with known redshifts the situation is different, because the fittings still allow one single Gaussian

curve. This result can be easily explained by selection effects - it is well-known that the observational determination of the redshifts in the Swift data sample is easier for the long bursts due to observational strategies (simply, it is more complicated to detect and to follow the afterglows of short GRBs (Gehrels et al. 2005)).

Concerning the third intermediate subgroup the whole sample also supports its existence; from seven tests six ones gave significances below 5%. Hence, strictly speaking, the third subclass does exist and the probability of the mistake for this claim is not higher than $x\%$, where $2.52 < x < 5.41$. This result is in accordance with the expectation, once a comparison with the BATSE database is provided. As it was said in Introduction, for the BATSE database the first evidence of third subgroup came from this χ^2 method, and hence also for the Swift database this test should give positive support for this subgroup, if the two datasets are comparable. It is the key result of this article that this expectation is fulfilled. Our study has shown that the classical χ^2 fitting - in combination with F-test - may well work also in the Swift database (similarly to the BATSE database (Horváth 1998)).

Horváth et al. (2008) confirmed the third subgroup in the Swift dataset by the maximum likelihood (ML) method. Our significance between 2.52% and 5.41% is weaker than the 0.46% significance obtained by Horváth et al. (2008), which is expectable, because the ML method is a stronger statistical test. This is seen from new two studies, too: the ML test on the databases of RHESSI (Rípa et al. 2009) and BeppoSAX (Horváth 2009) satellites, respectively, confirmed the existence of the third intermediate subclass; on the other hand, the χ^2 test either did not give a high enough significance for RHESSI data (Rípa et al. 2009) or was not used for BeppoSAX data at all (Horváth 2009).

It can also be expected that the mean $\log T_{90}$ for the intermediate group should be much higher in the Swift database due to the different redshift distributions (Band 2006, Jakobsson et al. 2006, Bagoly et al. 2006). The mean value for the BATSE's intermediate subgroup is 0.64 (Horváth 1998), but here the value is between 1.02 and 1.64. Also Horváth et al. (2008) obtained a similar value (1.107). Hence, also the typical durations are in accordance with the expectations.

The sample with no redshift did not find the third subgroup. This result can be explained by the smaller number of objects in the sample. The sample with known redshifts is strongly biased by selection effects, and here even the existence of the short subgroup was in doubt - hence, it seems to be hopeless to obtain some conclusions concerning the third subgroup.

5. Conclusions

Since the χ^2 fitting of the GRB duration distribution and the F-test were successfully used in the work Horváth 1998 (presenting the first evidence of the existence of three GRB subgroups), we proceed identically, but with the Swift's data.

The results may be summarized in the following four points:

1. Concerning the short and long subgroups all is in accordance with the expectation: they are detected also in the Swift database and - in addition - in the Swift database the weight of the short subgroup is smaller, which can be

well explained by the Swift's higher effective sensitivity to the softer bursts.

2. The whole sample of 388 objects gives support for three subgroups, because from seven fittings of the whole sample six ones confirmed the existence of the intermediate subgroup on a smaller than 5% significance level. Hence, concerning the Swift database, the situation is similar to the BATSE dataset - although our significances are weaker than $> 0.02\%$ of Horváth (1998).

3. The samples with and without known redshifts separately are either not enough populated, or strongly biased. Hence, no far reaching conclusions can be drawn from them.

4. Similarly to the BATSE database, here it is shown again that the classical χ^2 test - in combination with F-test - is also effective for the Swift GRB sample.

Acknowledgements. Thanks are due to valuable discussions with Z. Bagoly, L.G. Balázs, I. Horváth and P. Veres. This study was supported by the GAUK grant No. 46307, by the OTKA grants No. T48870 and K77795, by the Grant Agency of the Czech Republic grant No. 205/08/H005, and by the Research Program MSM0021620860 of the Ministry of Education of the Czech Republic. The useful remarks of the referee, C. Guidorzi, are kindly acknowledged.

References

- Bagoly, Z., Mészáros, A., Horváth, I., Balázs, L.G. & Mészáros, P. 1998, *ApJ*, 498, 342
- Bagoly, Z., Csabai, I., Mészáros, A., Mészáros, P., Horváth, I., Balázs, L.G. & Vavrek I. 2003, *A&A*, 398, 919
- Bagoly, Z., Mészáros, A., Balázs, L.G., Horváth, I., Klose, S., Larsson, S., Mészáros, P., Ryde, F., Tusnády 2006, *A&A*, 453, 797
- Balázs, L.G., Bagoly, Z., Horváth, I., Mészáros, A. & Mészáros, P. 2003, *A&A*, 401, 129
- Band, D.L., Ford, L.A., Matteson, J.L., Briggs, M.S., Paciesas, W.S., Pendleton, G.N. & Preece, R.D. 1997, *ApJ*, 485, 747
- Band, D.L. 2006, *ApJ*, 644, 378
- Barthelmy, S.D., et al. 2005, *Nature*, 438, 994
- Chattopadhyay, T., Misra, R., Chattopadhyay, A.K. & Naskar, M. 2007, *ApJ*, 667, 1017
- Gehrels, N., et al. (Swift team) 2005, http://heasarc.gsfc.nasa.gov/docs/swift/archive/grb_table/
- Hakkila, J. et al. 2000, *ApJ*, 538, 165
- Horváth, I. 1998, *ApJ*, 508, 757
- Horváth, I. 1999, *J. Korean Astron. Soc.*, 35, S629
- Horváth, I. 2002, *A&A*, 392, 791
- Horváth, I. 2003, in *Statistical Challenges in Modern Astronomy III.*, ed. E. D. Feigelson, & G. Jogesh Babu, (Springer, Berlin) 439
- Horváth, I., Balázs, L.G., Bagoly, Z., Ryde, F. & Mészáros, A. 2006, *A&A*, 447, 23
- Horváth, I., Balázs, L.G., Bagoly, Z. & Veres, P. 2008, *A&A*, 489, L1
- Horváth, I. 2009, *ASS*, in press; *astro-ph/0905.0860*
- Jakobsson, P., et al. 2006, *A&A*, 447, 897
- Kendall, M.G., & Stuart, A. 1973, *The Advanced Theory of Statistics*, Charles Griffin & Co. Ltd., London & High Wycombe
- Meegan, C.A., et al. 2001, *Current BATSE Gamma-Ray Burst Catalog*, <http://gammaray.msfc.nasa.gov/batse/grb/catalog>
- Mészáros, A., Bagoly, Z., Horváth, I., Balázs, L.G. & Vavrek, R. 2000, *ApJ*, 539, 98
- Mukherjee, S., Feigelson, E. D., Babu, G. J., Murtagh, F., Fraley, C. & Raftery, A. 1998, *ApJ*, 508, 314
- Norris, J.P. 2002, *ApJ*, 579, 386
- Rajaniemi, H.J. & Mähönen, P. 2002, *ApJ*, 566, 202
- Ramirez-Ruiz, E. & Fenimore, E.E. 2000, *ApJ*, 539, 712
- Řípa, J., Mészáros, A., Wigger, C., Huja, D., Hudec, R. & Hajdas, W. 2009, *A&A*, 498, 399
- Trumpler, R.J. & Weaver, H.F. 1953, *Statistical Astronomy*, University of California Press, Berkeley

Table 4. Swift GRBs with no measured redshifts; Part I.

<i>GRB</i>	T_{90} <i>sec</i>	<i>fluence</i> 10^{-7} erg/cm^2	<i>peak - flux</i> $\text{ph}/(\text{cm}^2 \text{ sec})$
090201	83.0	300.00	14.70
090129	17.5	21.00	3.70
090123	131.0	29.00	1.70
090118	16.0	4.00	<i>n/a</i>
090113	9.1	7.60	2.50
090111	24.8	6.20	0.90
090107 <i>A</i>	12.2	2.30	1.10
081230	60.7	8.20	0.70
081228	3.0	0.89	0.60
081226 <i>A</i>	0.4	0.99	2.40
081221	34.0	181.00	18.20
081211 <i>A</i>	3.5	1.30	0.80
081210	146.0	18.00	2.50
081203 <i>B</i>	23.4	21.00	<i>n/a</i>
081128	100.0	23.00	1.30
081127	37.0	4.90	0.60
081126	54.0	33.00	3.70
081109 <i>A</i>	190.0	36.00	1.10
081104	59.1	20.00	1.00
081102	63.0	23.00	1.40
081101	0.2	0.62	3.60
081025	23.0	19.00	1.30
081024 <i>A</i>	1.8	1.20	1.10
081022	160.0	25.00	0.60
081017	320.0	14.00	0.07
081016 <i>B</i>	2.6	0.99	0.50
081012	29.0	11.00	1.00
081011	9.0	1.60	0.40
080919	0.6	0.72	1.20
080916 <i>B</i>	32.0	6.30	0.60
080915 <i>B</i>	3.9	9.90	8.50
080915 <i>A</i>	14.0	2.30	0.50
080905 <i>A</i>	1.0	1.40	1.30
080903	66.0	14.00	0.80
080822 <i>B</i>	64.0	1.70	0.06
080802	176.0	13.00	0.30
080727 <i>C</i>	79.7	52.00	2.30
080727 <i>B</i>	8.6	31.00	7.60
080727 <i>A</i>	4.9	1.30	0.30
080725	120.0	37.00	2.30
080723 <i>A</i>	17.3	3.30	0.90
080714	33.0	25.00	4.20
080703	3.4	2.00	1.00
080702 <i>B</i>	20.0	5.00	0.50
080702 <i>A</i>	0.5	0.36	0.70
080701	18.0	7.10	2.20

Table 5. Swift GRBs with no measured redshifts; Part II.

<i>GRB</i>	T_{90} <i>sec</i>	<i>fluence</i> 10^{-7} erg/cm^2	<i>peak - flux</i> $\text{ph}/(\text{cm}^2 \text{sec})$
080623	15.2	10.00	2.00
080613B	105.0	58.00	2.70
080602	74.0	32.00	2.90
080524	9.0	2.90	0.40
080523	102.0	8.80	0.50
080517	64.6	5.60	0.60
080515	21.0	20.00	3.90
080506	150.0	13.00	0.40
080503	170.0	20.00	0.90
080426	1.7	3.70	4.80
080409	20.2	6.10	3.70
080405	40.0	12.00	<i>n/a</i>
080328	90.6	94.00	5.50
080325	128.4	49.00	1.40
080320	14.0	2.70	0.60
080319D	24.0	3.20	0.10
080319A	64.0	48.00	1.20
080315	65.0	1.40	0.04
080307	125.9	8.70	0.40
080303	67.0	6.60	1.40
080229A	64.0	90.00	5.70
080218B	6.2	5.10	3.10
080218A	27.6	6.30	1.40
080212	123.0	29.00	1.20
080207	340.0	61.00	1.00
080205	106.5	21.00	1.40
080130	65.0	7.70	0.20
080129	48.0	8.90	0.20
080123	115.0	5.70	1.80
080121	0.7	0.30	<i>n/a</i>
071129	420.0	35.00	0.90
071118	71.0	5.00	0.30
071112B	0.3	0.48	1.30
071110	19.0	0.76	0.40
071028B	55.0	2.50	1.40
071028A	27.0	3.00	0.30
071025	109.0	65.00	1.60
071018	376.0	10.00	0.20
071013	26.0	3.20	0.40
071011	61.0	22.00	1.70
071008	18.0	2.40	0.50
071006	50.0	1.40	13.00
071001	58.5	7.70	0.90
070923	0.1	0.10	2.40
070920B	20.2	6.60	0.80
070920A	56.0	5.10	0.30
070917	7.3	20.00	8.50
070913	3.2	2.50	1.40
070911	162.0	120.00	3.90

Table 6. Swift GRBs with no measured redshifts; Part III.

<i>GRB</i>	T_{90} <i>sec</i>	<i>fluence</i> 10^{-7} erg/cm^2	<i>peak - flux</i> $\text{ph}/(\text{cm}^2 \text{sec})$
070810B	80.0	0.12	1.80
070809	1.3	1.00	1.20
070808	32.0	12.00	2.00
070805	31.0	7.20	0.70
070731	2.9	1.60	1.20
070729	0.9	1.00	1.00
070721A	3.4	0.71	0.70
070714A	2.0	1.50	1.80
070704	380.0	59.00	2.10
070628	39.1	35.00	5.10
070621	33.3	43.00	2.50
070616	402.0	192.00	1.90
070612B	13.5	17.00	2.60
070610	4.6	2.40	0.90
070531	44.0	11.00	1.00
070520B	66.0	9.20	0.40
070520A	18.0	2.50	0.40
070518	5.5	1.60	0.70
070517	9.0	2.60	0.80
070509	7.7	1.70	0.70
070429B	0.5	0.63	1.80
070429A	163.0	9.20	0.40
070427	11.0	7.20	1.30
070420	77.0	140.00	7.10
070419B	236.5	75.00	1.40
070412	34.0	4.80	0.70
070406	0.7	0.45	0.70
070330	9.0	1.80	0.90
070328	69.0	89.00	4.20
070227	7.0	16.00	2.70
070224	34.0	3.10	0.30
070223	89.0	17.00	0.70
070220	129.0	106.00	5.88
070219	17.0	3.20	0.70
070209	0.1	0.11	2.40
070129	460.0	31.00	0.60
070126	51.0	1.60	0.20
070103	19.0	3.40	1.10
061222A	72.0	83.00	9.20
061218	4.1	0.20	0.41
061202	91.0	35.00	2.60
061126	191.0	72.00	9.80
061102	17.6	1.90	0.20
061028	106.0	9.70	0.70
061027	150.0	4.70	0.08
061021	46.0	30.00	6.10
061019	191.0	17.00	2.20
061006	130.0	14.30	5.36
061004	6.2	5.70	2.50
061002	17.6	6.80	0.80
060929	12.4	2.80	0.40
060923C	76.0	16.00	1.00
060923B	8.8	4.80	1.50
060923A	51.7	8.70	1.30
060919	9.1	5.50	2.20
060904A	80.0	79.00	4.90

Table 7. Swift GRBs with no measured redshifts; Part IV. **Table 8.** Swift GRBs with no measured redshifts; Part V.

<i>GRB</i>	T_{90} <i>sec</i>	<i>fluence</i> 10^{-7} erg/cm^2	<i>peak - flux</i> $\text{ph}/(\text{cm}^2 \text{ sec})$
060825	8.1	9.80	2.70
060813	14.9	55.00	9.00
060807	34.0	7.30	0.80
060805	5.4	0.74	0.30
060804	16.0	5.10	1.20
060801	0.5	0.81	1.30
060728	60.0	2.40	<i>n/a</i>
060719	55.0	16.00	2.30
060717	3.0	0.65	0.50
060712	26.0	13.00	1.70
060607 <i>B</i>	31.0	17.00	1.50
060602 <i>A</i>	60.0	16.00	0.50
060516	160.0	11.00	0.30
060515	52.0	14.00	0.80
060510 <i>A</i>	21.0	98.00	17.00
060507	185.0	45.00	1.30
060501	26.0	12.00	1.90
060428 <i>B</i>	58.0	7.20	0.60
060428 <i>A</i>	39.4	14.00	2.40
060427	64.0	5.00	0.30
060424	37.0	6.80	1.60
060421	11.0	12.00	3.00
0604131	50.0	36.00	0.90
060403	30.0	14.00	1.00
060323	18.0	5.70	0.80
060322	213.0	51.00	2.10
060319	12.0	2.70	1.10
060313	0.7	11.30	12.10
060312	43.0	18.00	1.50
060306	61.0	22.00	6.10
060223 <i>B</i>	10.2	16.00	2.90
060219	62.0	4.20	0.60
060211 <i>B</i>	29.0	4.70	0.70
060211 <i>A</i>	126.0	15.00	0.40
060204 <i>B</i>	134.0	30.00	1.30
060203	60.0	8.50	0.60
060202	203.7	24.00	0.50
060117	16.0	204.00	48.90
060111 <i>B</i>	59.0	16.00	1.40
060111 <i>A</i>	13.0	11.80	1.72
060110	17.0	14.00	1.90
060109	116.0	6.40	0.50
060105	55.0	182.00	7.50
060102	21.0	2.40	0.40
051227	8.0	2.30	0.97
051221 <i>B</i>	61.0	11.30	0.54
051213	70.0	8.00	0.51
051210	1.4	0.83	0.75
051117 <i>B</i>	8.0	1.40	0.46
051117 <i>A</i>	140.0	46.00	0.93
051114	2.2	1.32	0.73
051113	94.0	26.00	2.40
051105 <i>A</i>	0.3	0.20	2.00
051021 <i>B</i>	47.0	9.10	0.63
051016 <i>A</i>	22.0	8.80	1.60
051012	13.0	2.90	0.60
051008	16.0	58.00	5.50
051006	26.0	12.80	1.90
051001	190.0	18.00	0.51

<i>GRB</i>	T_{90} <i>sec</i>	<i>fluence</i> 10^{-7} erg/cm^2	<i>peak - flux</i> $\text{ph}/(\text{cm}^2 \text{ sec})$
050925	0.1	0.75	1.50
050922 <i>B</i>	250.0	26.00	1.02
050916	90.0	11.00	0.69
050915 <i>B</i>	40.0	34.00	2.34
050915 <i>A</i>	53.0	8.80	0.80
050911	16.0	3.01	1.31
050906	0.1	0.07	1.15
050827	49.0	21.20	1.86
050822	102.0	26.10	2.47
050820 <i>B</i>	13.0	21.20	4.06
050819	36.0	3.52	0.39
050815	2.8	0.92	0.56
050801	20.0	3.12	1.47
050721	39.0	30.80	3.08
050717	86.0	61.70	6.34
050715	52.0	14.40	1.07
050713 <i>A</i>	70.0	52.50	4.78
050712	48.0	11.00	0.55
050701	22.0	13.60	2.77
050607	26.5	6.05	0.99
050528	10.8	4.40	1.23
050509 <i>A</i>	11.6	3.38	0.88
050502 <i>B</i>	17.5	4.72	1.43
050422	59.2	6.15	0.57
050421	10.3	1.18	0.44
050418	83.0	53.90	3.80
050416 <i>B</i>	5.4	11.30	5.85
050412	26.0	5.66	0.49
050410	43.0	43.00	1.80
050326	29.5	90.50	12.40
050306	160.0	120.00	3.64
050219 <i>B</i>	27.0	164.00	25.40
050219 <i>A</i>	23.0	42.10	3.61
050215 <i>B</i>	8.0	2.33	0.68
050215 <i>A</i>	6.0	7.29	0.51
050202	0.1	0.33	2.98
050128	13.8	51.70	7.59
050124	4.1	12.30	5.57
050117	169.0	91.20	2.40
041228	62.0	36.10	1.65
041226	15.0	3.23	0.34
041224	235.0	75.30	2.95
041223	107.0	171.00	7.49
041220	5.0	3.82	1.83
041219 <i>C</i>	40.0	20.00	1.50
041219 <i>B</i>	30.0	<i>n/a</i>	10.00
041219 <i>A</i>	520.0	1000.00	25.00
041217	7.5	65.70	4.40

Table 9. Swift GRBs with known redshifts; Part I.

<i>GRB</i>	<i>T</i> ₉₀ <i>sec</i>	<i>fluence</i> 10^{-7} erg/cm^2	<i>peak - flux</i> $\text{ph}/(\text{cm}^2 \text{ sec})$	<i>z</i>
090205	8.8	1.90	0.50	4.6749
090102	27.0	0.68	5.50	1.5477
081222	24.0	48.00	7.70	2.7467
081203A	294.0	77.00	2.90	2.1000
081121	14.0	41.00	4.40	2.5120
081118	67.0	12.00	0.60	2.5800
081029	270.0	21.00	0.50	3.8474
081028A	260.0	37.00	0.50	3.03800
081008	185.5	43.00	1.30	1.96775
081007	10.0	7.10	2.60	0.52950
080928	280.0	25.00	2.10	1.6910
080916A	60.0	40.00	2.70	0.68900
080913	8.0	5.60	1.40	6.57000
080906	147.0	35.00	1.00	2.00000
080905B	128.0	18.00	0.50	2.37400
080810	106.0	46.00	2.00	3.35000
080805	78.0	25.00	1.10	1.50500
080804	34.0	36.00	3.10	2.20225
080721	16.2	120.00	20.90	2.59650
080710	120.0	14.00	1.00	0.84500
080707	27.1	5.20	1.00	1.23000
080607	79.0	240.00	23.10	3.03600
080605	20.0	133.00	19.90	1.63980
080604	82.0	8.00	0.40	1.41600
080603B	60.0	24.00	3.50	2.69000
080520	2.8	0.55	0.50	1.54500
080516	5.8	2.60	1.80	3.20000
080430	16.2	12.00	2.60	0.75850
080413B	8.0	32.00	18.70	1.10000
080413A	46.0	35.00	5.60	2.43300
080411	56.0	264.00	43.20	1.03000
080330	61.0	3.40	0.90	1.51000
080319C	34.0	36.00	5.20	1.95000
080319B	50.0	810.00	24.80	0.93700
080310	365.0	23.00	1.30	2.42580
080210	45.0	18.00	1.60	2.64100

Table 10. Swift GRBs with known redshifts; Part II.

<i>GRB</i>	<i>T</i> ₉₀ <i>sec</i>	<i>fluence</i> 10^{-7} erg/cm^2	<i>peak - flux</i> $\text{ph}/(\text{cm}^2 \text{ sec})$	<i>z</i>
071227	1.8	2.20	1.60	0.3835
071122	68.7	5.80	0.40	1.14
071117	6.6	24.00	11.30	1.331
071112C	15.0	30.00	8.00	0.82
071031	180.0	9.00	0.50	2.692
071021	225.0	13.00	0.70	5.0
071020	4.2	23.00	8.40	2.1435
071010B	35.7	44.00	7.70	0.947
071010A	6.0	2.00	0.80	0.98
071003	150.0	83.00	6.30	1.0185
070810A	11.0	6.90	1.90	2.17
070802	16.4	2.80	0.40	2.45
070724A	0.4	0.80	1.00	0.457
070721B	340.0	36.00	1.50	3.626
070714B	64.0	7.20	2.70	0.92
070612A	370.0	110.00	1.50	0.617
070611	12.0	39.00	0.80	2.04
070529	109.0	26.00	1.40	2.4996
070521	37.9	80.00	6.70	0.553
070508	21.0	200.00	24.70	0.82
070506	4.3	2.10	1.00	2.31
070419A	116.0	5.60	2.80	0.97
070411	101.0	25.00	1.00	2.954
070318	63.0	23.00	1.60	0.838
070306	210.0	55.00	4.20	1.497
070208	48.0	4.30	0.90	1.165
070110	85.0	16.00	0.60	2.352
061222B	40.0	22.00	1.50	3.355
061217	0.3	0.46	1.30	0.827
061210	85.0	11.00	5.30	0.41
061201	0.8	3.30	3.90	0.111
061121	81.0	137.00	21.10	1.314
061110B	128.0	13.00	0.40	3.44
061110A	41.0	11.00	0.50	0.758
061007	75.0	450.00	15.30	1.2615
060927	22.6	11.00	2.80	5.6
060926	8.0	2.20	1.10	3.208
060912	5.0	13.00	8.50	0.937
060908	19.3	29.00	3.20	2.43
060906	43.6	22.10	2.00	3.685
060904B	192.0	17.00	2.50	0.703
060814	146.0	150.00	7.40	0.84
060729	116.0	27.00	1.40	0.54
060714	115.0	30.00	1.40	2.71
060708	9.8	5.00	2.00	2.3
060707	68.0	17.00	1.10	3.43

Table 11. Swift GRBs with known redshifts; Part III.

<i>GRB</i>	T_{90} <i>sec</i>	<i>fluence</i> 10^{-7} erg/cm^2	<i>peak – flux</i> $\text{ph}/(\text{cm}^2 \text{ sec})$	<i>z</i>
060614	102.0	217.00	11.60	0.1275
060607A	100.0	26.00	1.40	3.082
060605	15.0	4.60	0.50	3.76
060604	10.0	1.30	0.60	2.68
060526	13.8	4.90	1.70	3.21
060522	69.0	11.00	0.60	5.11
060512	8.6	2.30	0.90	0.4428
060510B	276.0	42.00	0.60	4.9
060505	4.0	6.20	1.90	0.089
060502B	90.0	0.40	4.40	0.287
060502A	33.0	22.00	1.70	1.51
060418	52.0	81.00	6.70	1.4895
060223A	11.0	6.80	1.40	4.41
060210	255.0	77.00	2.80	3.91
060206	7.0	8.40	2.80	4.048
060123	900.0	3.00	0.04	1.099
060116	113.0	26.00	1.10	5.3
060115	142.0	18.00	0.90	3.53
060108	14.4	3.70	0.70	2.03
051221A	1.4	11.60	12.10	0.547
051111	47.0	39.00	2.50	1.549
051109B	15.0	2.70	0.50	0.08
051109A	36.0	21.00	3.70	2.346
051016B	4.0	1.70	1.32	0.9364
050922C	5.0	17.00	7.36	2.198
050908	20.0	4.91	0.70	3.3459
050904	225.0	50.70	0.66	6.29
050826	35.0	4.51	0.43	0.297
050824	25.0	2.92	0.52	0.83
050820A	26.0	40.10	2.50	2.61335
050814	65.0	18.30	0.75	5.3
050813	0.6	0.43	0.92	1.80
050803	85.0	22.30	1.08	0.422
050802	13.0	22.00	2.65	1.71
050730	155.0	24.20	0.57	3.9669
050724	3.0	11.80	3.29	0.2575
050603	13.0	76.30	27.60	2.821
050525A	8.8	156.00	42.30	0.606
050509B	0.04	0.13	1.33	0.225
050505	60.0	24.90	1.81	4.27
050416A	2.4	4.31	4.97	0.6535
050406	3.0	0.81	0.38	2.44
050401	33.0	85.50	12.60	2.9
050319	10.0	6.25	1.45	3.24
050318	32.0	13.10	3.20	1.44
050315	96.0	32.30	1.98	1.949
050223	23.0	6.40	0.70	0.58775
050126	26.0	8.60	0.70	1.29